

~~UNCLASSIFIED~~
UNCLASSIFIED

PUBLICLY RELEASABLE

Per George Biggs FSS-16 Date: 4-18-96
By Madeline Lyjars CIC-14 Date: 8-7-96

~~SECRET~~

Classification changed to UNCLASSIFIED
by authority of the U. S. Atomic Energy Commission,

Per H. J. Carroll 2-1-56
By REPORT LIBRARY V. Martin
2-24-56

L A - 82

[REDACTED]

May 18, 1944

This document contains 51 pages

FISSION CROSS SECTION OF 25 FOR 0.01 TO 1000 EV. NEUTRONS

WORK DONE BY:

- E. E. Anderson
- L. S. Lavatelli
- B. D. McDaniel
- R. E. Sutton

REPORT WRITTEN BY:

- E. E. Anderson
- L. S. Lavatelli
- B. D. McDaniel
- R. E. Sutton

LOS ALAMOS NATL. LAB. LIBS.
3 9338 00329 0292

[REDACTED]

~~SECRET~~

UNCLASSIFIED

UNCLASSIFIED

ABSTRACT

A measurement has been made of the variation of the ratio $\sigma_p(25)/\sigma(B)$ for neutrons of energy from 0.01 ev to 1000 ev. The neutron energy was measured by the time of flight method. The most striking characteristic of the variation is the appearance of resonances in the fission cross section. With the resolution used, several narrow resonances between thermal energies and about 10 ev were observed. Between 10 and 1000 ev there appeared large variations in the cross section many volts wide which probably consist of groups of unresolved resonances. The only resonance resolved was one at 0.25 ev, whose width is of the order of 0.2 ev. The resonances at 1.0, 3.3, and 9.5 ev, though not completely resolved, are fairly narrow, of the order of a volt or so at most. From 0.01 ev to 2 ev, the average value of the ratio $\sigma_p(25)/\sigma(B)$ decreases by a factor of about four. From 5 ev to 50 ev it rises by about a factor of 10 and does not fall again for at least a thousand ev. If boron follows the $1/v$ law for the $(n - \alpha)$ process up to 1000 ev, then $\sigma_p(25)$ increases by about 2.7 in going from 0.025 ev to 1000 ev.

A transmission measurement for 25 has also been made for neutrons in the energy interval from 0.01 to 1 ev. The 25 total absorption cross section shows the same general characteristics as the fission cross section. The ratio of total absorption cross section to the fission cross section apparently increases rather rapidly with increasing energy of the neutrons. Because of certain considerations relating to experimental conditions, it is not conclusive that this observed increase is real. The absorption cross section at 0.025 ev was measured to be 650 ± 16 barns.

UNCLASSIFIED

-3-

FISSION CROSS SECTION OF 25 FOR 0.01 TO 1000 EV. NEUTRONS

FISSION CROSS SECTION OF 25

INTRODUCTION

This experiment is a study by the time of flight method of the ratio of the fission cross section of 25, $\left[\sigma_f(25) \right]$, to the $\sigma(B)$ cross section of boron, $\sigma(B)$, in the energy region extending from 0.01 to 1000 ev.

Absorption measurements at Chicago¹⁾ give a value of 645 barns for the absorption cross section of 25 at a neutron velocity of 2200 m/sec or about 0.025 ev. Measurements at Wisconsin²⁾ show that the fission cross section is essentially constant and equal to 1.6 b above 0.5 Mev. Between 0.15 and 0.5 Mev the cross section varies approximately as $1/v$. The value in this region is about twelve times the value obtained by a $1/v$ extrapolation of the cross section at thermal energies.

The group directed by J. H. Williams³⁾ has studied $\sigma_f(25)/\sigma(B)$ between 1.5 ev and 400 ev by a boron absorption method. They found that this ratio increases by a factor of 3.3 from 2 ev to 200 ev. The work described in this report was undertaken to verify these measurements by an independent method with considerably better resolution.

-
- 1) CP-1088
 - 2) CF-618
 - 3) LA-46

APPARATUS

The cyclotron was used as the primary neutron source. Hydrogenous material was used to reduce the energy of as many of these neutrons as possible to the region below 1000 ev. A slow neutron velocity spectrometer was used to select neutrons of the desired energy. A 25 fission chamber and two BF_3 chambers were used as detectors.

The velocity spectrometer has been described in earlier published literature^{4,5,6)} except for some minor modifications. As in the case with the earlier experiments with this equipment, measurements were made of the time lag between the time the arc was turned on in the cyclotron and the time of production of neutrons at the target. It was found that this time lag was about 25 μsec . The lag was due mostly to the time necessary to accelerate the deuterons in the cyclotron and so depended on the dee voltage, on the radial position of the target, and on the tuning of the cyclotron. Since it was difficult to hold conditions sufficiently steady to keep the time lag constant to within 1 μsec , a tracking circuit was used which kept the neutron burst at the same position in time by varying the time at which the arc was modulated, so that the time lag was compensated.

-
- 4) B. D. McDaniel, Absorption of Slow Neutrons by Indium, Ph.D. Thesis Cornell University, 1943
 - 5) G. P. Baker, B. D. McDaniel, M. G. Holloway and R. F. Bacher, The Transmission of Thick Cadmium. CP-305, 1942
 - 6) Bacher, Baker and McDaniel. Experiments with a Slow Neutron Velocity Spectrometer, C-25

-5-

To prevent neutrons other than those originating at the source from arriving at the detector, a 12 inch I.D. collimator was used. This collimator consisted of a cylinder of B_4C having a thickness of 1.3 gm/cm^2 inside a cylinder of paraffin 5 cm thick. One end of this was placed as near as possible to the internal probe of the cyclotron, and the slow neutron source was placed at the same end. The detector was put in the collimator several meters from the source.

The slow neutron source used depended upon the region of the spectrum under investigation. For energies below about 1 ev two types of sources were used. One was a slab of paraffin 5 cm thick. The time of flight distribution of neutrons from this source detected in a BF_3 chamber is shown in Fig. 1, curve (a). This distribution will hereafter be denoted as the BF_3 spectrum. There are two disadvantages to this source. One is that the steep slope in the region of a few tenths of a volt accentuates any errors in timing and in the positions of the source or detector. The second disadvantage is that the mean life of thermal neutrons in the source is of the order of $100 \mu\text{sec}$ so that the resolution is badly distorted when working in the thermal region at short distances.

To overcome these disadvantages, a source was used which consisted of a 5 cm thick tank containing a solution of 7 gm of B_2O_3 per liter of water. In addition, on the side of the tank next to the detector a B_2O_3 absorber, approximately $.1 \text{ gm/cm}^2$ thick, was placed. The boron in the tank reduced the mean life to about $50 \mu\text{sec}$, while the boron absorber outside the tank reduced the height of the thermal peak. The BF_3 spectrum for this source is shown by curve (b) in Fig. 1. It is seen from the figure that the


-6-

low energy tail of the distribution function does not extend to as great a time of flight as it does in the case of the normal paraffin source. This permits the use of a higher repetition frequency when the boron source is being used since it is not necessary to wait as long for most of the low energy neutrons to get by the detector before repeating the cycle.

In order to investigate the region above 1 ev, it was desirable further to increase the repetition rate. This was accomplished by placing 0.9 gm per cm² of Cd between the paraffin source and the detector. Curve (c) of Fig. 1 shows the resulting spectrum. It is seen that the Cd absorbs practically all neutrons with a time of flight greater than about 130 μ sec/m allowing the use of a much higher repetition rate than would otherwise be possible.

For the region around 1000 ev, the use of a 0.65 gm/cm² B₄C absorber with the paraffin source + Cd permitted the use of a repetition frequency two and one half times greater than that which would be possible without it. The thickness of the slowing down material for the above described sources was determined experimentally to give the maximum number of neutrons in the region below 1000 ev.

One of the detectors was a EF₃ ionization chamber. This chamber consisted of an outside cylinder, 6.25 cm in diameter, and an axial rod, 1.5 mm diameter, both at about seventeen hundred volts negative to ground. Coaxial with this assembly, and insulated from it was a cylindrical collector assembly made up of seven rods placed on a circle of 4 cm diameter. The end through which the neutrons entered was closed by a dural (24ST) cap, 3/32 inch thick.



-7-

The chamber was filled with BF_3 at atmospheric pressure and had a useful length of about 20 cm. This chamber contained enough boron to have a 30 per cent absorption for thermal neutrons. The result of this absorption is that the chamber is less sensitive to low energy neutrons than it should be. At 0.025 ev the effect was calculated to be 15 per cent. As a check on this effect, a second BF_3 chamber was used. The dimensions, except for the length, were the same as for the one described above. This "thin chamber" had an active length of 13 cm, and contained about $1/5$ atmosphere of BF_3 and $4/5$ atmosphere of argon. The calculated decrease in the sensitivity at 0.025 ev is 2.5 per cent for this chamber. Comparison of the spectra measured by the two chambers indicated that the calculated correction factor was in good agreement with the experimental results. Electron collection was used in both chambers, with a collection time of the order of 1 μsec .

The 25 chamber was enclosed by a copper cylinder 25 cm in diameter and 30 cm long. The cover over the front end was a plate of $3/32$ inch dural. The electrode assembly consisted of 14 aluminum foils, 0.0008 inches thick, 20.5 cm in diameter, mounted on circular rings and arranged parallel to the face of the chamber, separated by 1 cm. Alternate plates were connected electrically, one set served as collector, the other as the high voltage electrode, maintained at 400 volts negative with respect to ground. The shell of the chamber was grounded. Enriched uranium oxide, for which the ratio of 25 to 28 was about 1 to 8, was sprayed onto each side of the foils to a thickness of 1 mg per cm^2 of uranium. There was a total of 7.74 gm of uranium in the chamber, of which about 0.89 gm was 25. The chamber was filled

with argon at atmospheric pressure. Electron collection was also used in this chamber with a collection time of the order of 1 μ sec.

None of the chambers had a plateau, but, since the measurements taken were the ratio of counts for neutrons of a specified energy range to the total counts, small changes in sensitivity had no effect on the results.

PROCEDURE

The method of taking measurements is described below. The 25 chamber was placed in the collimator at a certain distance from the source. The delays in time between the production of the neutron burst and the various detector sensitivity intervals were adjusted to correspond to the neutron times of flight to be investigated. The number of counts, C, in each of the sensitive intervals, and the total numbers of counts, T, were recorded. This was repeated for the BF_3 chamber. These data give the ratio $\sigma_f(25)/\sigma(B)$ for the times of flight considered, except for a constant which depends on the shape of the spectrum as measured by the chambers. This may be seen as follows:

$$\left(\frac{C}{T}\right)_{25} = \frac{Nf(\tau) \sigma_f(25) F_{25} \Delta_{25}}{\int_{\text{all } \tau} Nf(\tau) \sigma_f(25) F_{25} d\tau} = \frac{f(\tau) \sigma_f(25) \Delta_{25}}{\int f(\tau) \sigma_f(25) d\tau} \quad (1)$$

where N is the total number of neutrons arriving at the chamber during the run. Δ is the "on time". The function $f(\tau)$ is the fraction of N which lie in the time of flight interval between τ and $\tau + d\tau$. F_{25} is the geometrical sensitivity of the chamber. A similar expression holds for the BF_3 chamber:

-9-

$$\left(\frac{C}{T}\right)_B = \frac{f(\tau) \sigma(B) \Delta_B}{\int f(\tau) \sigma(B) d\tau} \quad (2)$$

If the same resolution was used with both chambers, then $\Delta_{25} = \Delta_B$.

Thus

$$R = \frac{(C/T)_{25}}{(C/T)_B} = \frac{\sigma_f(25)}{\sigma(B)} \times \frac{\int f(\tau) \sigma(B) d\tau}{\int f(\tau) \sigma_f(25) d\tau} \quad (3)$$

The ratio of the integrals depends only on the shape of the spectrum as measured by the chambers; this does not change unless the source is changed.

The chambers were interchanged frequently during measurements on each energy setting so that any changes in spectrum would be detected. At least two runs were made between each interchange of the chambers, each run of length sufficient to give about 100 counts on the slowest counter.

The equations (1) and (2) above indicate that (C/T) is a function of the integral $\int f(\tau) \sigma(\tau) d\tau$. If the spectrum changes, (C/T) for a given energy will change by a different fraction for the two detectors, since $\sigma_f(25)/\sigma(B)$ is not a constant with respect to neutron energy. As a result, when measurements of $\sigma_f(25)/\sigma(B)$ are made with different sources it is necessary to apply a normalization to make the data correspond. The procedure to measure this normalization factor is indicated by the following considerations,

Consider first the 25 chamber. Equation (1) gives,

$$\left(\frac{C}{T}\right)_{25} = \frac{f(\tau) \sigma_f(25) \Delta_{25}}{\int f(\tau) \sigma_f(25) d\tau}$$

-10-

For a different source $f(\tau)$ will be different, say $f'(\tau)$, so

$$\left(\frac{C}{T}\right)_{25}' = \frac{f'(\tau) \sigma_f(25) \Delta'_{25}}{\int f'(\tau) \sigma_f(25) d\tau}$$

Similarly, for the BF_3 chamber, we have for one source

$$\left(\frac{C}{T}\right)_B = \frac{f(\tau) \sigma(B) \Delta_B}{\int f(\tau) \sigma(B) d\tau}$$

and for the other source,

$$\left(\frac{C}{T}\right)_B' = \frac{f'(\tau) \sigma(B) \Delta'_B}{\int f'(\tau) \sigma(B) d\tau}$$

Combining these equations, with the assumption that $\Delta_{25} = \Delta_B$,

$$\Delta'_{25} = \Delta'_B$$

gives

$$\frac{\left(\frac{C}{T}\right)_{25} / \left(\frac{C}{T}\right)_B}{\left(\frac{C}{T}\right)_{25}' / \left(\frac{C}{T}\right)_B'} = \frac{\left[\int f(\tau) \sigma(B) d\tau \right] / \left[\int f'(\tau) \sigma(B) d\tau \right]}{\left[\int f(\tau) \sigma_f(25) d\tau \right] / \left[\int f'(\tau) \sigma_f(25) d\tau \right]} = N$$

or if we let

$$R = \left(\frac{C}{T}\right)_{25} / \left(\frac{C}{T}\right)_B \quad R' = \left(\frac{C}{T}\right)_{25}' / \left(\frac{C}{T}\right)_B'$$

and let N be defined by the above equation, then

$$R = R'N$$

-11-

N was determined in the following manner. The untimed total counts for one chamber for each source were measured. The ratio of these counts is given by the following equation:

$$\frac{F_{25} N_{25} \int f(\tau) \sigma_f(25) d\tau}{F'_{25} N'_{25} \int f'(\tau) \sigma_f(25) d\tau}$$

F_{25} and F'_{25} , the sensitivities of the 25 chamber for the two sources, are not energy dependent. N_{25} and N'_{25} are the number of neutrons arriving at the chamber for the two runs. F_{25} and F'_{25} were kept equal during the measurements, and N_{25} and N'_{25} were kept at a certain ratio by a neutron monitor. The same measurements were made for the BF_3 chamber, keeping the ratio N_B/N'_B the same as for the 25 measurement. The ratio of the results of these two sets of measurements gives the number N .

When the cyclotron arc voltage is turned off the neutron intensity does not drop to zero because of the acceleration of ions which are formed in places other than in the arc. Thus, when making timed measurements, it was necessary to measure the unmodulated part of the neutron beam and to correct the data for it. This background was measured by turning off the arc voltage and recording the total number of counts in an interval of several minutes, making certain that the cyclotron remained in tune during the background run. The timed counts were corrected by a fraction of this background corresponding to the fraction of the total time for which a given channel

-12-

was sensitive. Since the background increased with increasing gas pressure, the pressure was kept constant and as low as possible. In most cases the background was less than 1 percent of the timed counts.

A further possible source of background is leakage into the collimator of neutrons which do not originate at the source. The magnitude of this background was measured by placing in the source end of the collimator a plug of about 30 cm of paraffin and 1 gm/cm² of B₂O₃ and taking a timed run at the energy region of interest. This indicated that it was necessary to place additional paraffin around that part of the collimator near the cyclotron. A plug consisting of 1 gm/cm² of B₂O₃ was placed in the collimator behind the detector to prevent neutrons from entering there. After these precautions were taken, the background was measured to be less than one percent of the timed counts. A shield of paraffin and boron was placed behind the source to prevent the neutrons, which are scattered around inside the water tanks which surround the cyclotron, from entering the source and thus arriving at the detector at a time not corresponding to their energy. This was shown to be necessary by the fact that the 36 ev iodine resonance was sharper with the shield in place than without it.

In some cases it was necessary to measure and correct for the recycling background -- that is for the counts measured in one cycle which were due to slow neutrons from the preceding cycle. This measurement was made in the following manner. For making the background measurement a repetition period was set up which was at least twice as long as the period to be used in the experiment. Six of the sensitive intervals were set at a time after the neutron burst corresponding to the energy to be investigated,

while the other six were set up later than this by one period of the frequency to be used in the experiment. This gave the ratio of the counts due to recycling to the total number of counts for the experiment. The correction was usually less than one percent.

If the neutron pulse and the detector sensitivity pulse were perfectly square the sensitivity curve plotted on a time of flight scale would have the form of an isosceles triangle. If τ is the time between the beginning of the arc "on-time" and the beginning of the detector "on-time", and if the arc "on-time" and detector "on-time" are of δ μ sec. duration, the base of this triangle is 2δ ; the highest energy neutrons detected have a time of flight of $\tau - \delta$ μ sec. and the lowest energy neutrons have a time of flight of $\tau + \delta$ μ sec; seventy-five percent of the neutrons detected fall in the time of flight region between $\tau - \delta/2$ and $\tau + \delta/2$.

However, various factors enter to distort this theoretical shape. One is that the number of ions from the arc, or at least the intensity of the neutron pulse, does not go to zero as rapidly as does the arc voltage. Similarly, the intensity of the pulse rises more slowly than does the arc voltage. The effect of this is to broaden the sensitivity curve and to make it less sharp. This was demonstrated experimentally by the use of a proton recoil chamber. The chamber was placed as close as possible to the cyclotron target. The proton recoil pulses from the neutrons were amplified by an amplifier having a rise time of about 0.05 μ sec. and a decay time of 0.7 μ sec. The output of this amplifier was connected to the vertical plates of an oscilloscope. The sweep of the oscilloscope was synchronized to the arc repetition frequency. Since the neutron intensity at the chamber is

very great, recoil pulses are not observed individually but only the current of these pulses is observed. This gives a picture of the neutron intensity in the pulse from the cyclotron target. Observation of this pulse indicated that the neutron pulse was at least $1 \mu\text{sec.}$ longer than the voltage pulse applied to the arc. This width depended greatly on the gas pressure in the cyclotron, increasing from about $8 \mu\text{sec.}$ to $12 \mu\text{sec.}$ when the total pressure changed by 30 percent.


Data on the experimental resolution were also obtained in the following manner. A timed run was taken on neutrons of essentially zero time of flight with $5 \mu\text{sec.}$ "on times". A fast neutron chamber was placed at such a distance that the individual pulses could be counted. If the intensity of the neutron pulse rose to maximum value and fell to zero in infinitely short times, it is easily seen that plotting the number of counts in each timed counter against the time difference between the beginning of the sensitive time of the counter and the arc "on time" would give a triangle exactly similar to the resolution triangle. The curve resulting from this experiment is actually the mirror image of the resolution curve plotted on a time of flight axis. This may be seen from the fact that the fastest neutrons detected in a time of flight measurement must be those which originate at a time near the end of the neutron pulse.

The results of this experiment for $5 \mu\text{sec.}$ "on-times" are shown in figure 2. The high energy tail extends about $2.5 \mu\text{sec.}$ beyond the theoretical sensitivity curve. For "on times" above 10 or $20 \mu\text{sec.}$, the distortion of the resolution curve due to the imperfect neutron pulse is negligible.

Distortion of the resolution curve can arise from the finite length of the chamber. This results in an uncertainty in the distance of flight, or a corresponding uncertainty in the time of flight. This uncertainty in the time of flight is simply given by the product of the length of the chamber and the time of flight per meter of the neutron in which one is interested. It is apparent that this uncertainty in the time of flight increases with decreasing energy. Since the thing that concerns the resolution is the uncertainty in the time of flight per meter, this product must be divided by the distance of flight in order to obtain an index of the resolution. This effect of decreasing the resolution is then greatest for low energies and short distances of flight. With the exception of one set of observations, this resolution distortion was negligible. In the special case, the altered resolution function is shown accompanying the results. (See fig. 4).

For measurements in the thermal region, the greatest distortion by far arises from the decay time of slow neutrons in the source. In about $2 \mu\text{sec.}$ after the fast neutron pulse from the cyclotron enters the slow neutron source, equilibrium of the neutrons in the source is reached, with a maximum in the time of flight distribution curve for neutrons emitted from the source at about $300 \mu\text{sec/m}$ plotted on a time of flight scale. This equilibrium distribution retains its shape while the neutron intensity decays with a half life of about $110 \mu\text{sec.}$ for the paraffin source and of $50 \mu\text{sec.}$ for the source consisting of the boron solution.

Thus there are neutrons of energies varying from 0.01 ev up to



about 0.1 ev being emitted for several hundred μ sec. after the primary neutron burst. Hence if the detector becomes sensitive at a time after the primary burst corresponding to the time of flight of a low energy neutron, it will detect also neutrons of higher energies which were emitted later than the one of low energy. Since after one to two μ sec. later than the primary burst, there are almost no neutrons in the source of energy greater than 0.1 ev, measurements above this region are not affected by mean life. For thermal measurements the distortion becomes smaller as the distance is increased, so that it is preferable to work at large distances. For most of the work which was done in the thermal energy region, the distance of flight was so great that even for a 100 μ sec. mean life, the distortion of the resolution function was small.

RESULTS

The measurements may be conveniently broken into five groups. Most of these groups contain several sets of measurements. The ranges covered by these groups are (1) 0.01 to 0.2 ev., (2) 0.1 to 2.0 ev., (3) 0.5 to 100 ev., (4) 15 to 250 ev., (5) 120 to 1000 ev. The experimental conditions under which the measurements were made are listed in Table I.

It was shown in the section above that the quantity

$$R = (C/T)_{25} / (C/T)_B$$

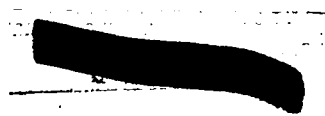
gives only the relative variation of $\sigma_f(25) / \sigma(B)$. The absolute value of R depends on the shape of the primary neutron spectrum. As a conse-

-17-

quence, in order to compare the results of the various measurements, it is necessary to multiply them by the appropriate normalization factors N . Figures 3, 4, 7, 8 and 9 are curves of R against time of flight per meter for the various regions and are not normalized. (Region 1b was multiplied by 1.03 to fit it to 1a, c and d). In figure 10, which includes the results for all five regions, each region has been normalized to measurement 1a, and then $\sigma_p(25)/\sigma'(B)$ has been adjusted to equal unity at 0.025 ev. Thus to plot the curves of figures 3, 4, 7, 8 and 9, on figure 10, they must be multiplied by 1.08, 1.26, 1.36, 1.19 and 2.34 respectively. See the appendix for the computation of these factors. Probable errors have not been indicated on the curves. However, the shape is determined in all regions by points each arising from at least five hundred counts for each chamber.

Figure 3 shows a plot of the values of R determined from the measurements of group 1. The abscissa is a time of flight axis in units of microseconds per meter. At various points along this axis, the corresponding energy in ev. is also marked. The measurements 1a and 1b were taken with the thick boron chamber and were corrected for the absorption in the chamber. For measurements of 1c, both the thick and the thin boron chambers were used. The thick chamber corrections were applied and the measurements with the boron chambers were combined to obtain the BF_3 spectrum. In measurement 1d, the thin chamber was used. The triangles drawn along the abscissa indicate the resolutions used.

The measurements of group 2 were all made using the boron source and thick boron chamber. The results of the three measurements using



-18-

different resolutions are given in figure 4. The scattering of the points is greater than would be expected from the probable errors and is perhaps in part instrumental.

Group 3 involves three sets of measurements with different resolutions. All were taken using the normal paraffin source and cadmium around the detector. Only the thicker of the two boron chambers was used. When the data were taken, the 25 chamber was always 10 cm. further away from the source than the boron chamber. Since the spectra were observed using the same timing scheme for both chambers, the observed points do not occur at the same place on the time of flight scale when it is reduced to microseconds per meter. Because of this, it was not possible to take point by point ratios of the 25 and BF_3 spectra, but instead, the two spectra were plotted separately. They are shown in figures 5 and 6 respectively. Smooth curves were drawn to fit the points and in the high energy region, the 4.85 meter data was weighted most heavily. Point by point ratios were then taken from the smooth curves. These ratios are plotted in figure 7.

It will be observed that there is scattering, greater than that to be expected from statistical reasons, among the points in figure 5. This seems to be due to some systematic error in the timing, since a slight translation of the time axis for one set of points relative to the others gives much better agreement. This probably results directly from the fact that no tracking circuit was used to keep the time lag constant, and it was not known at the time these data were taken that the time lag varied so greatly. A change of time lag of only $5 \mu\text{sec.}$ for the data taken at 1.85 m is needed to explain the greatest shift which one would need to produce optimum agreement. It was

felt that the need for additional information in this region was not sufficiently great to merit further work to resolve these discrepancies.

The measurements in group 4 were made up of two sets taken at different times but with the same resolution. The beam tracking circuit was used. The results are shown in figure 8.

The results of the measurements of group 5 are shown in figure 9. These measurements were made using the normal paraffin source, the boron recycling shield and Cd around the detectors. The tracking circuit was also used for this measurement. In order to determine the time lag and the shape of the resolution function, a fast neutron spectrum was obtained as described earlier and as shown in figure 2. Because of the high repetition rate and because the boron recycling shield was not sufficiently thick to prevent recycling, a 10 percent recycling correction had to be applied to the boron data, however none was necessary for the 25 data because in the region where recycled neutrons are troublesome the cross section of 25 is so small as to make the correction negligible.

The measurements for time of flight less than 2 μ seconds (about 1300 ev) are not to be relied upon because of possible uncertainties in the timing. For example, the point at about 0.6 μ sec. (10,000 ev) probably averages in the effect of some neutrons of several million volts, resulting in an increase in the value of R because of the fission of the 23 which is present in the sample.

In addition to these groups of timed measurements, another set of timed measurements was taken in order to determine the ratio of the average value of R at about 100 ev. to the value at thermal energies. To do this the boron source was used and the distance to the detector was 7.6 m. The

-20-

thick boron chamber was used. The "on-times" were $40 \mu\text{sec.}$ and the repetition rate 208.5 cps. The arc position was monitored by the tracking circuit. One of the detector channels was set for a mean time of flight of $8 \mu\text{sec.}$ per meter which corresponds to about 83 ev. The extreme ends of the sensitivity interval were at 580 and 31 ev. Six other channels were set about a mean time of flight of $265 \mu\text{sec.}$ per meter or 0.075 ev. The averages for these six channels were obtained and compared to the values for the 83 ev. channel. The usual corrections were made to these results. The corrected results are given below.

$$R_{83}/R_{0.075} = 2.94 \pm 5\%$$

The variation of $\sigma_f(25)/\sigma(B)$ with energy over the region from 0.01 ev. to 1000 ev. is shown in the composite figure 10. The abscissa is a logarithmic energy axis. The fit between the measurements of groups 2 and 3 is not very good. No good reason can be advanced for the lack of agreement. It may be that the disagreement results from the fact that several pieces of data must be fitted together at different points to establish a continuous curve. In addition, as may be seen from the scattering of the points in figure 6, the value of R in the region from 0.5 to 1.2 ev. is not very well determined. Of course this region is probably of much less interest than is the relation between the measurements of group 1 and group 4. This latter relation is rather well established by the measured normalization factors.

The most significant features of the variation of the cross section are the following. In the thermal region the ratio of the cross section decreases slowly with increasing energy. The ratio R decreases by about

(9 ± 3) percent going from 0.01 to 0.05 ev. A resonance of about 0.2 ev. width appears at about 0.25 ev. This resonance seems to be relatively well resolved, but in spite of this fact the change in cross section is rather small. At about 1 volt another resonance occurs. This resonance is not well resolved as is also the case with all higher energy resonances. At 3 volts another weak resonance occurs. At about 7 volts the cross section ratio rises very rapidly by about a factor of ten. Though there are some considerable unresolved fluctuations, the cross section increases only slowly in the region from about 30 volts on up to 1000 ev. In the region of 1000 ev., the average value of R is about 2.75 times the value at 0.025 ev.

CONCLUSIONS

There are a few significant conclusions to be drawn from these results. The first and perhaps most important is that fission is a resonance phenomenon. Though it had been suspected before, this is the first conclusive evidence on this point. From the data in the region of 0.025 ev. it is evident that these resonances may be quite narrow. Actually this particular resonance is of the order of 0.2 ev. wide. Although none of the higher resonances have been resolved, it is apparent that they also must be fairly narrow. The large rise in the average ratio of cross sections in the region of 7 volts is rather interesting because it does not fall again to some lower value at higher energy. This is probably to be explained by the fact that narrow resonances are certainly not resolved in this region, and the change in the average cross section is caused by a change in the average level density.

If one makes the reasonable assumption that boron follows the $1/v$ law



-22-

as high as 1000 ev., then we see that the average value of $v\sigma_f$ for 25 increases by about 2.7 in going from 0.025 ev. to 1000 ev.

TRANSMISSION OF 25

INTRODUCTION

It was found desirable to measure the transmission of enriched uranium samples by the time of flight method. One reason for this was to see if the general characteristics observed in the fission cross section could also be observed in the total capture cross section determined by transmission. A second reason arose as a result of the small widths of the fission levels which were found in the measurements discussed in the first part of this report. At least some of the fission resonances have widths comparable to those expected for capture with gamma ray emission. Because of this, it seems possible that there is an appreciable probability for capture with the emission of a gamma ray as well as capture with fission. If the probability for gamma capture varied with energy in a radically different manner from that for capture with fission, by studying the total capture cross section and comparing it to the fission cross section, positive evidence for appreciable gamma capture would be obtained.

Recent unpublished experiments by Fermi and also Bailey have obtained positive evidence for existence of gamma capture. Their work consisted of independent measurements of fission and total capture cross section.

METHOD

The general techniques for making transmission measurements are



-23-

described by Baker and Bacher ¹⁾. The only essential difference in the method of making the measurements from that described in the published article is in the measurement of the total transmission of the samples. Instead of relying upon the stability of the neutron intensity during the measurements, a stable fission counter was used as a monitor of intensity.

The geometrical arrangement for the experiment is described below. The neutron source used was the boron water tank with the B_2O_3 tray which was described in the earlier section of this paper. The large paraffin and boron carbide collimator was also used. A BF_3 chamber was placed inside the large collimator at 7.6 m from the source. The chamber was immediately surrounded by a small boron carbide collimator of density 1.0 g/cm^2 which extended 75 cm. in front of the chamber. The diameter of the collimator at the aperture was 2 inches. The transmission sample to be studied was placed over this aperture.

A sample of uranium oxide, enriched in 25, was used. The amount of 25 contained in the sample was 13.74 percent by weight of the total amount of uranium present. The entire sample of the oxide weighed 309.6 gms., but was divided into two parts. These two parts, designated as #1 and #2 contained approximately ~~one~~^{TWO} third and ~~two~~^{ONE} thirds respectively of the total amount. The samples were placed in cylindrical aluminum containers having an inside diameter of 2.50 inches. The end caps of the containers were 1/32 inch duraluminum.


In addition to the enriched samples, two other samples, #3 and #4, were made up of normal tuballoy oxide. These were placed in containers similar to those for the enriched samples. The normal samples had almost exactly the

same weight of material in them as did samples 1 and 2. The transmission of each of the normal samples was also measured in order to permit a correction to the cross section determined from the enriched samples for the scattering and capture from the relatively large amount of ^{28}Al present in the enriched samples. In order to compensate for the thickness of aluminum which was in the beam when the absorber was in, aluminum blanks of equal thickness were placed in the beam when the "absorber out" measurements were made. In Table II the weights of the various samples are tabulated.

The observations were carried out in two parts. One part was made in the thermal range using the thin absorber, sample #2, and the corresponding unenriched sample #4. The resolution used was $200\ \mu\text{sec}$. "on time" for the arc and detector. The second part of the measurements was carried out using the enriched samples #1 and #2 together, and unenriched samples #3 and #4. The "on time" for detector and arc was $50\ \mu\text{sec}$. The measurements extended up to a little more than 1 volt. The timed observations were made using a rotating sequence of enriched sample, normal sample, and aluminum disk. For the low energy region, two complete cycles of this sequence were made, while for the higher energy points, 5 cycles were made. The total transmission of each sample was made relative to the aluminum plates.

RESULTS

The results of the total transmission measurements are given in Table III. These measurements are of equal accuracy. By using the percentage mean deviation from the average, for all observations, the probable error of the average of a set was computed to be about 1.5 percent.



The absolute transmissions for the various absorbers are shown in Figs. 11, 12, 13 and 14. The transmission is plotted as a function of time of flight per meter. The probable errors shown are the statistical errors associated with the timed counts only and do not include the error in the total transmission.

The shape of the lines drawn through the points in Figs. 12 and 14 have been chosen so as to be in agreement with certain assumptions and conditions. It is assumed that the scattering cross section of uranium and oxygen are constant, while the cross section for capture of 28 and 25 vary, to a first approximation, as $1/v$. It is further assumed that these cross sections bear the ratio to one another at 0.025 ev. as the values tabulated below. However these are not assumed to be the absolute values, but the absolute values are adjusted to provide the best fit to the data.

28 scattering	8.0	barns per atom of uranium in normal tuballoy
28 capture	3.0	
25 capture	4.6	
oxygen scattering	3.3	barns per atom of oxygen

It is felt that the curve of Figs. 12 and 14 are a far better determination of the cross section of normal tuballoy than the individual experimental points, consequently values were taken off these curves to determine the cross section for normal uranium oxide.

The general absorption law is;

$$T = e^{-\sigma n}$$

where T is the transmission for a given cross section per atom (σ) and n

given number of atoms (n) per cm^2 . Let $\alpha = \sigma n$ then

$$T = e^{-\alpha}$$

In Fig. 15 are plotted the cross sections determined from the observations. The cross sections are given per atom of uranium in each sample.

In order to obtain the 25 capture cross section from the data, the following procedure is used.

$$\text{Define } \varphi = \sigma_c(25) + \sigma_s(25) - \sigma_c(28) - \sigma_s(28)$$

where $\sigma_s(25)$, and $\sigma_c(25)$, are the scattering and capture cross sections respectively for 25, and where $\sigma_s(28)$, and $\sigma_c(28)$, are the corresponding cross sections for 28. Then it is easily shown that:

$$\varphi = (\alpha - \alpha') / (n - n')$$

where α , α' are absorption coefficients for the enriched sample and normal sample respectively, and n and n' are the numbers of atoms of 25 in the two samples. If one makes the following assumptions a value for the capture cross section of 25 may be obtained. Assume $\sigma_s(28) = \sigma_s(25)$ and that $\sigma_c(28)$ at 0.025 ev. is 3.0 barns and varies as $1/v$. The above discussion also assumes that there are equal numbers of atoms of uranium in the enriched and the corresponding unenriched sample. This is true to about 0.2 percent.

The values for $\sigma_c(25)$ based on these considerations is plotted in Fig. 16. The value of $\sigma_c(25)$ v normalized arbitrarily to unity at 0.025 ev. is shown in Fig. 17. The smooth curve shown is drawn to fit the experimental points from the transmission measurements while the dotted curve is the curve for the corresponding region obtained from the fission measurements reported

-27-

in the first section of this paper. Fig. 18 shows the value of $\sigma_c(25) v$ and $\sigma_f(25) v$ on an energy plot.

The value of the capture cross section at 0.025 ev. is determined from the curves to be 650 ± 16 barns.

DISCUSSION

It is seen that the general behavior of the capture cross section determined by transmission is quite similar to that of the fission cross section. However, the quantitative agreement between the two groups of measurements is not as good as would be expected if the energy dependence were the same for the two. This is especially true in the region of the resonance at 0.25 ev. where the difference between the two curves is about 30 percent.

It is possible of course that this indicates that gamma ray capture increases relative to capture for fission with increasing energy. However, it is to be considered that the transmission measurements were made in the presence of a large amount of scattering from the 28, making it more difficult to get good values for the 25 cross section. In the enriched sample, a scattering of about 9 barns per atom of uranium greater than that present in the normal sample would make the two curves have about the same energy dependence. As little as 0.4 percent by weight of water in the enriched sample would provide this additional amount of scattering. However after measuring the water content of the samples, it was deemed unlikely that more than 1/10 this amount was present. If the scattering cross section of 25 were about 6.5 times the scattering for 28, it would be sufficient to provide the addi-

tional 9 barns of scattering. The latter possibility is exceedingly unlikely.

The possibility of error in the measurements of the fission cross section in this region cannot be excluded. The cross section in this region was obtained from two sets of measurements which were joined together by fit. However, it is difficult to see how these measurements can be in error by so large an amount.

CONCLUSION

It seems that the conclusion to be drawn from this experiment is that the general behavior of the total capture cross section for ^{25}Pu is similar to that for the capture for fission, but quantitatively the behavior may be somewhat different. The measurements indicate that the ratio of the total capture cross section to the fission cross section increases by 40 percent in going from 0.025 ev. to 0.25 ev. It is felt that the present measurements are not sufficiently accurate to conclude definitely that this apparent increase is real, though it may be. A much more definite conclusion could be reached if the experiment could be repeated for both the fission and the transmission measurements. In the transmission measurements, a great decrease in the scattering background could be achieved if metal samples, instead of the oxide, could be used, and if a higher enrichment of ^{25}Pu in the sample could be attained.

APPENDIX A

NORMALIZATION OF FISSION MEASUREMENTS

Three normalization measurements were made. One of these was between measurements 5a and 4a. The second of these was between measurements 4a and 1a. The third was between measurements 4b and 1b. It is seen that two of these normalizations are between measurements of region 4 and region 1. The measured normalization factor to relate 4a to 1a was found to be 1.17 ± 10 percent. The normalization factor to relate 4b to 1b was found to be 1.08. However, in order to fit 1b to 1a, 1a was multiplied by 1.03 so that to relate 4b to the values plotted on Fig. 3, it is necessary to multiply (4b) by the factor 1.11 ± 5 percent. The agreement between the various factors indicates to some degree the precision of the measurements.

The error quoted for the first factor is based upon the mean deviation of several observations and upon geometrical changes which may possibly have occurred during the measurements involving both the normalization measurements and the timed runs with which they are associated. The geometry was most likely to be altered because of certain inconveniences which existed in making the exchange between types of spectra. In making the normalization measurement for the second factor, the possibility of altering the geometry during the course of the measurements was considerably reduced. In addition, the normalization runs were inter-meshed with the timed runs in such a way as to reduce the effect of changes in the geometry. The error quoted is based upon the mean deviations of several observations.

Two more values of this normalization factor can be obtained. One

of these is obtained by combining all the data of groups 1 to 4 into one curve. The segments are adjusted for the best fit of the values of R for overlapping regions of the spectrum. In order to obtain this fit, the curve of Fig. 3 must be multiplied by the factor 0.94. The estimated error of fit is 15 percent.

The final method for obtaining a normalization factor for these two regions is by utilizing the data which compares the value of R at 83 ev. directly to its value at 0.075 ev. As given above, $R_{83}/R_{0.075}$ is 2.94. The value of R_{83} represents the average of R over the resolution function used in the experiment.

The average of the curve in Fig. 8 over the resolution function yields the value 2.27. However the value of R at 0.075 ev. on the curve of Fig. 3 is 0.855. We wish to normalize the curve of Fig. 8 so that the average of the resolution function over the curve bears a ratio of 2.94 to the value of R for Fig. 3 at 0.075 ev. Thus in order to do this it is necessary to multiply the curve of Fig. 8 by the factor 1.11 ± 7 percent. This factor is obtained from the product of $2.94 \times 0.855/2.27$. The error is the statistical probable error associated with the factor.

We have now four values for the factor by which the curve of Fig. 8 must be multiplied to compare it to Fig. 3. These values are:

1.17	\pm	10	percent
1.11	\pm	5	"
0.94	\pm	15	"
1.11	\pm	7	"

After taking the weighted mean of these quantities we obtain the value 1.11 ± 4 percent.

For the region 5, we have two methods for determining the normalization factor. The first of these utilizes the normalization measurement between 5a and 4a. This value is 1.92. The second method makes use of fitting of curve 9 to curve 8. This gives a normalization value of 2.02. The average of these two values is 1.97. Therefore to compare Fig. 9 to Fig. 8, Fig. 9 should be multiplied by 1.97. In order to compare Fig. 9 to Fig. 3, Fig. 9 should be multiplied by 1.97×1.11 . This factor is 2.18 ± 5 percent.

The results of all the measurements are combined in the graph shown in Fig. 10. In addition to applying all the appropriate normalization factors to the data, all the measurements have been multiplied by 1.08 to adjust the value of R to unity at 0.025 ev. The measurements of group 4 and 5 have been normalized by the use of the factors found above, while groups 2 and 3 are adjusted for the best fit. To plot the data then, the curves of Figs. 3, 4, 7, 8 and 9 are multiplied by 1.08, 1.26, 1.36, 1.19 and 2.34 respectively. In Fig. 10, only the curves from the various figures have been shown. The abscissa is a logarithmic energy axis.

TABLE I

	Region	Source	Boron Detector	Distance (meters)	"On-time" (μ sec)	Frequency (cps)	Designat
1	0.01 to 0.2	Paraffin	thick	7.6	200	100	1a.
			thick	7.6	200	100	1b.
			thick and thin	7.6	200	100	1c.
			thin	7.6	250	200	1d.
2	0.1 to 2.0	Boron	thick	2.5	10	500	2a.
				2.5	20	500	2b.
				2.0	10	500	2c.
3	0.5 to 100	Paraffin and Cd	thick	1.85	5	2500	3a.
				2.85	10	2500	3b.
				4.85	10	1000	3c.
4	15 to 250	Paraffin and Cd	thick	7.6	10	1000	4a.
				7.6	10	1000	4b.
5	120 to 1000	Paraffin, Cd, and boron recycling shield	thick	7.6	5	2500	5a.

-33-

TABLE II

Diameter of sample = 2.500 inches

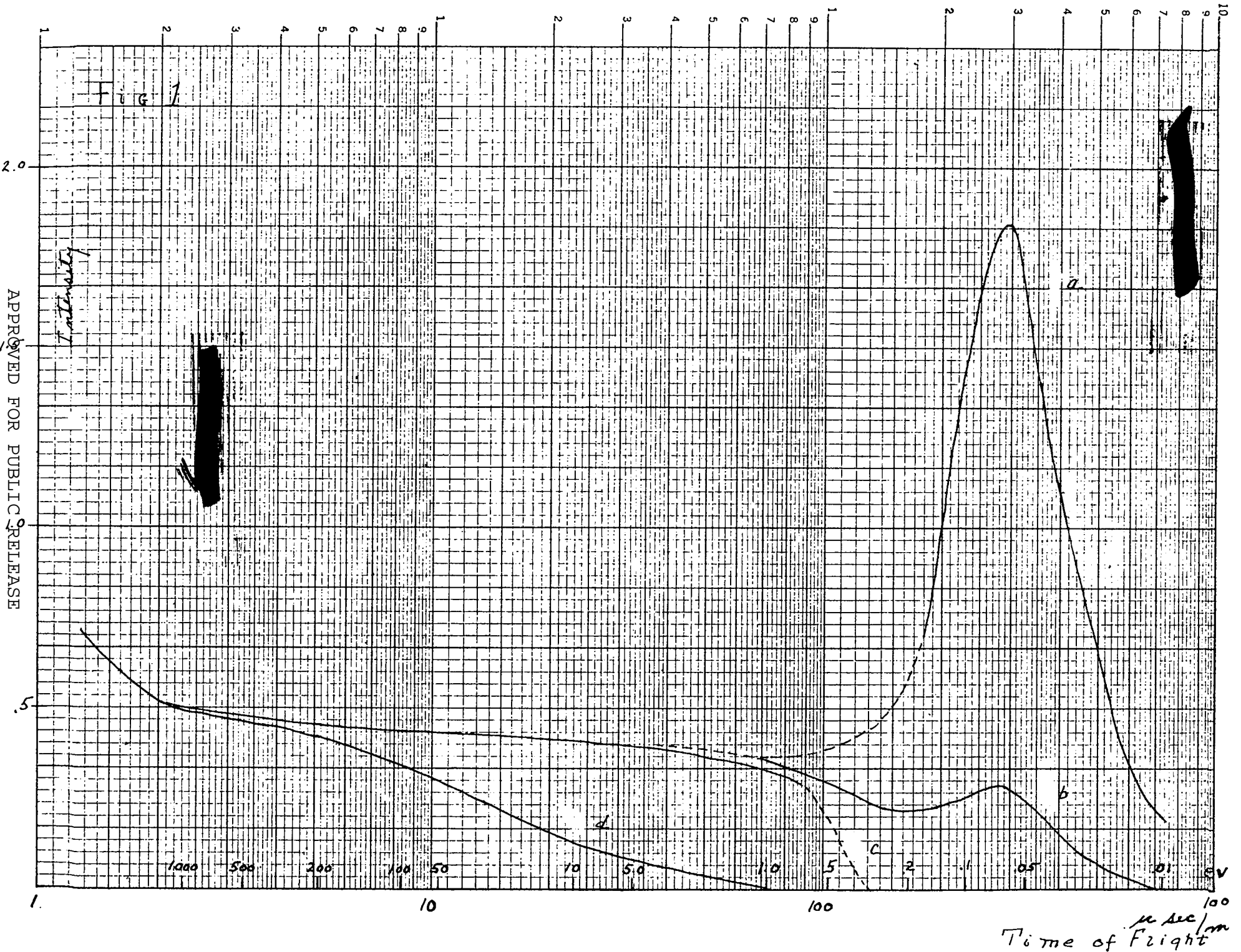
Area of sample = 31.66 sq. cm.

R = 6.29 by weight = 13.74% by weight

<u>No. of Sample</u>	<u>wt. of oxide</u>	<u>gms. oxide/sq. cm.</u>	<u>gms. Tu/sq. cm.</u>	<u>Atoms Tu/sq. cm.</u>
#1	206.48	6.522	5.531	14.11×10^{21}
#2	103.1	3.256	2.761	7.043×10^{21}
#3	206.5	6.522	5.531	14.08×10^{21}
#4	103.0	3.253	2.758	7.021×10^{21}

TABLE III

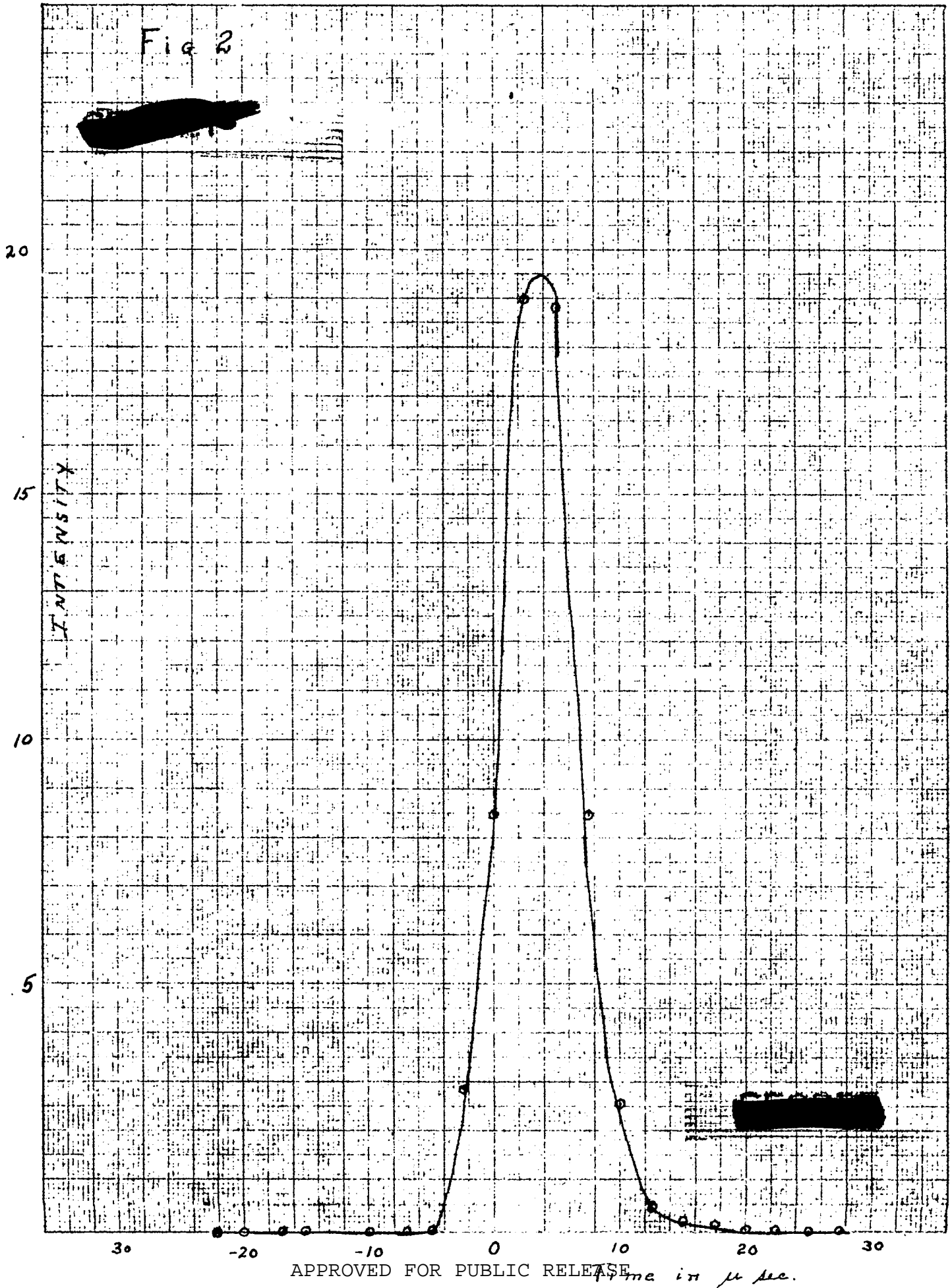
<u>Sample No.</u>	<u>Total Transmission</u>
1 and 2	.367 .368 .377 Average .371
2	.689 .741 .700 Average .710
3 and 4	.638 .630 Average .634
4	.861 .885 Average .873



APPROVED FOR PUBLIC RELEASE

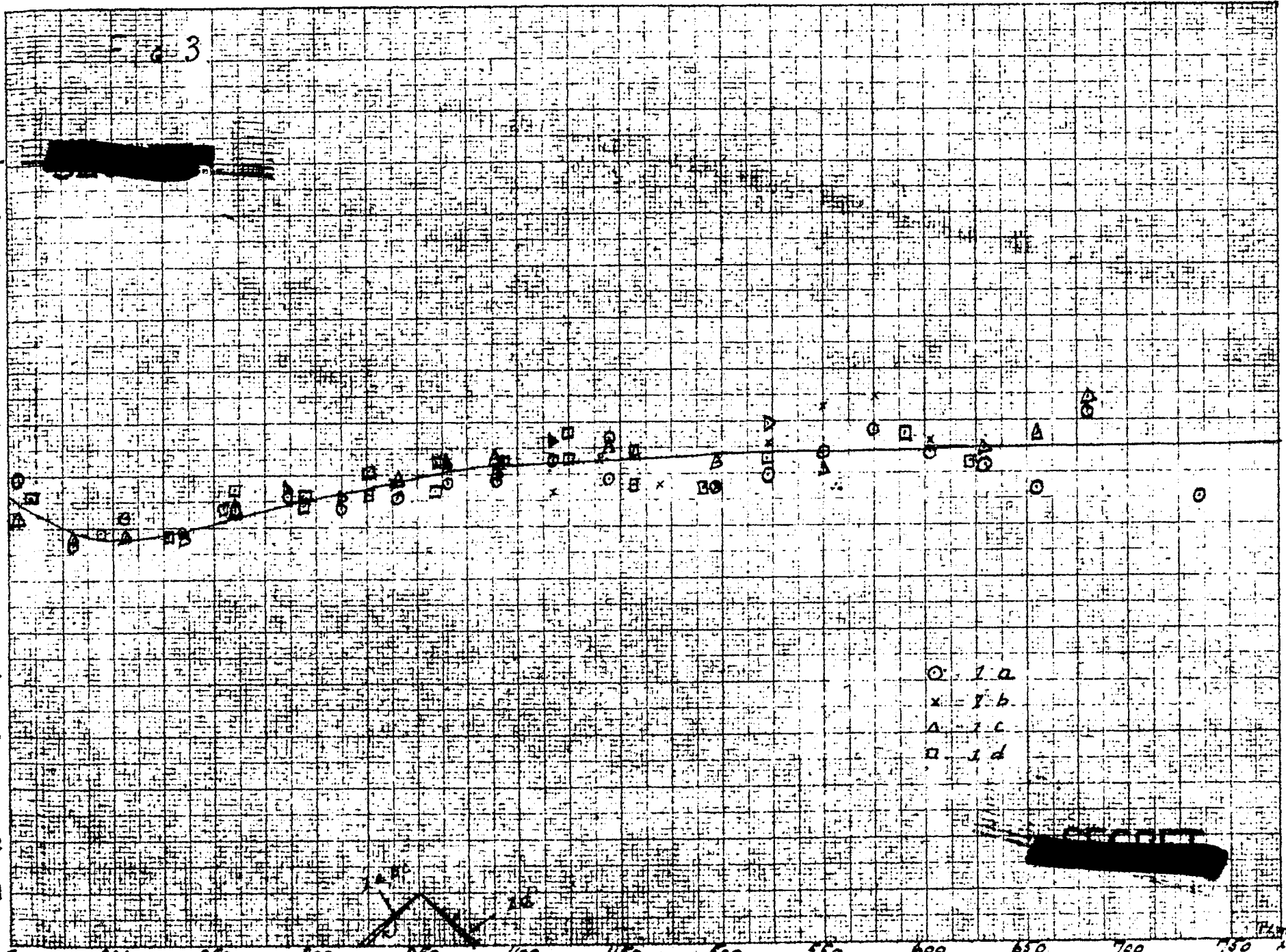
APPROVED FOR PUBLIC RELEASE

Fig 2



5/25/69

APPROVED FOR PUBLIC RELEASE



150 .23 200 .13 250 .088 300 .058 350 .043 400 .033 450 .026 500 .021 550 .017 600 .0145 650 .0122 700 .009 750 .0073

APPROVED FOR PUBLIC RELEASE

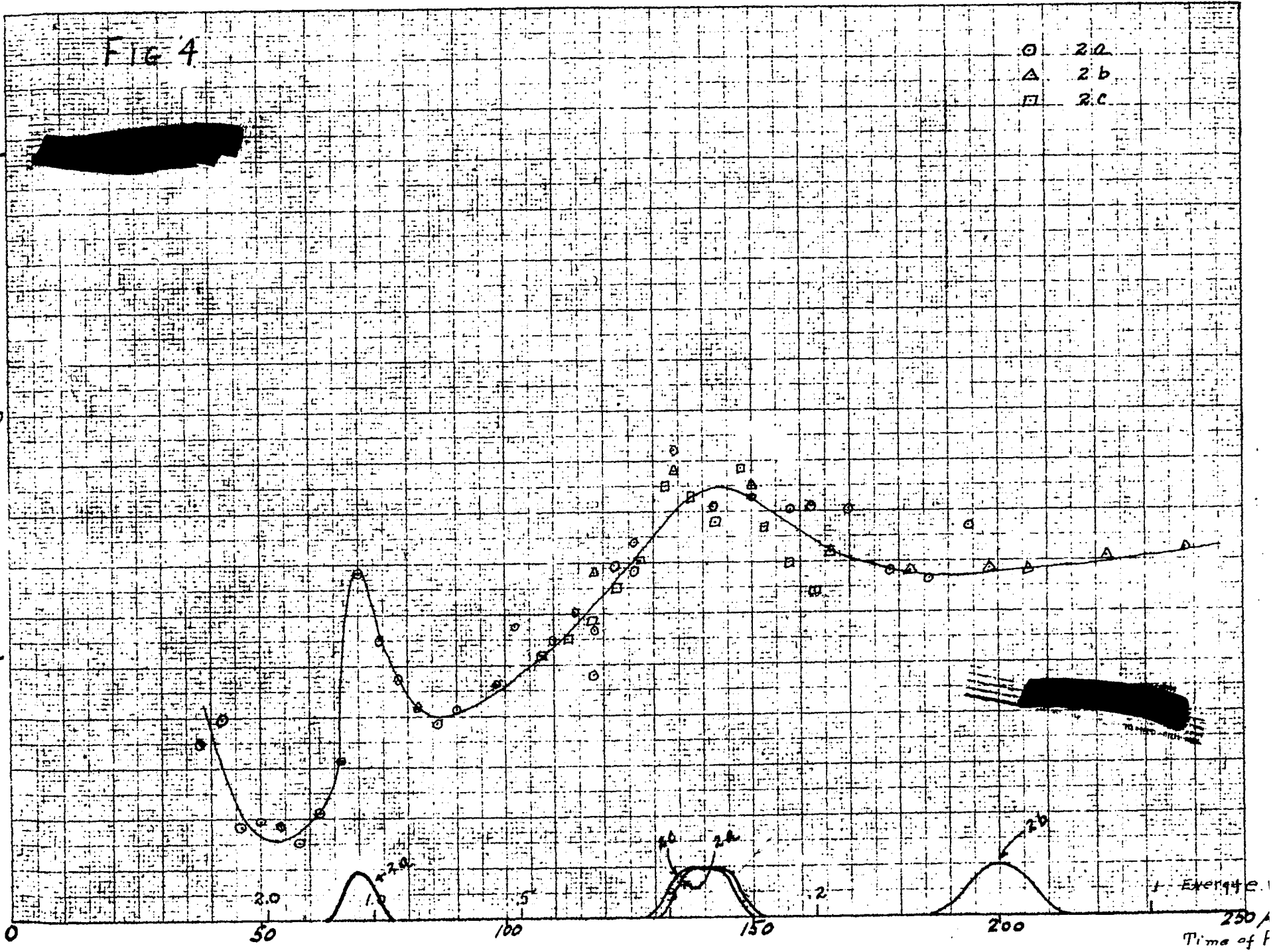
FIG 4

$\frac{G_{25}}{G_B}$

○ 2.0
△ 2.0
□ 2.0

APPROVED FOR PUBLIC RELEASE

APPROVED FOR PUBLIC RELEASE



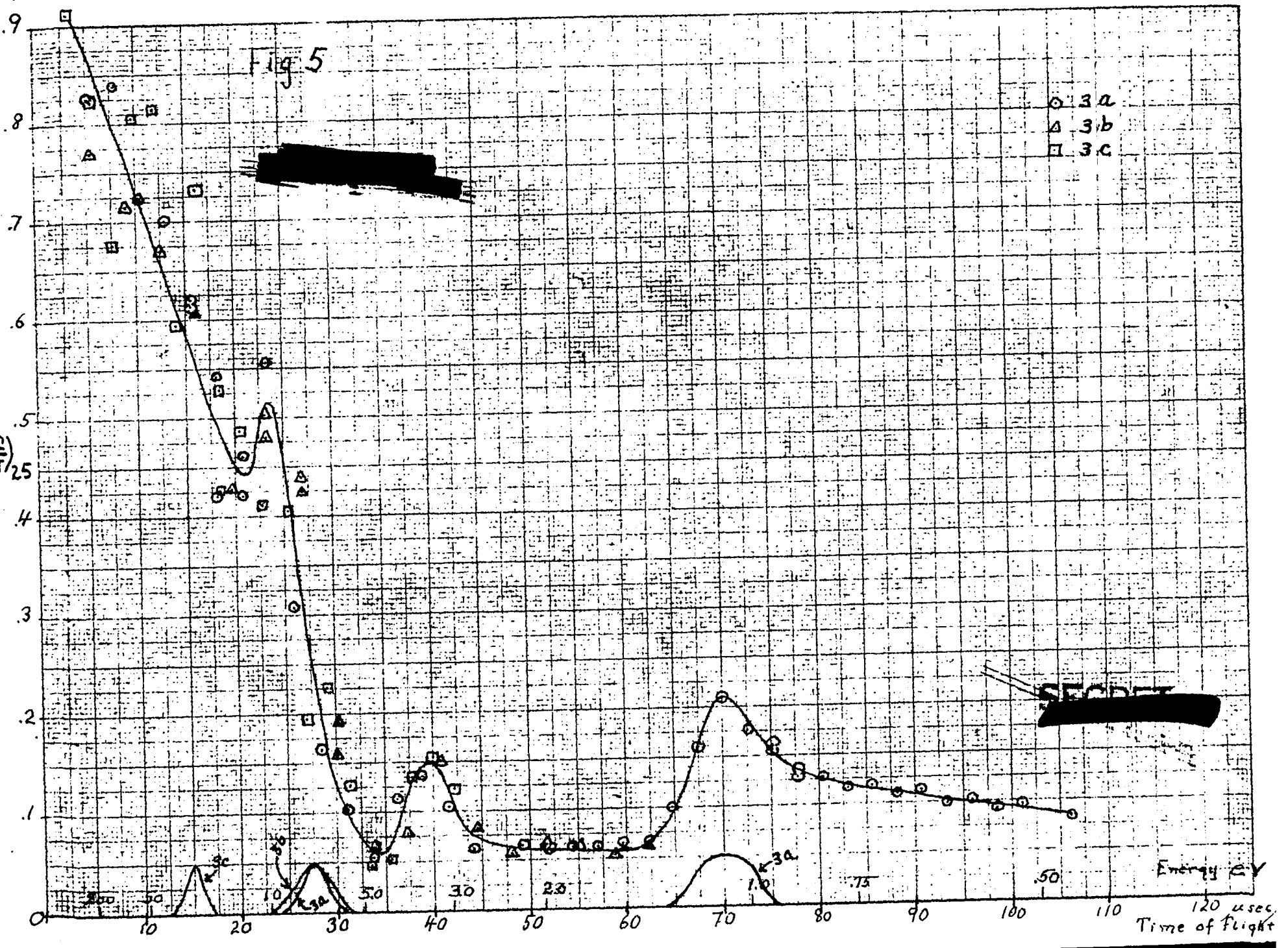
Example 1
250 /
Time of f

$\left(\frac{C}{T}\right)_{25}$

TABLE 1
CROSS SECTION DATA

APPROVED FOR PUBLIC RELEASE

APPROVED FOR PUBLIC RELEASE



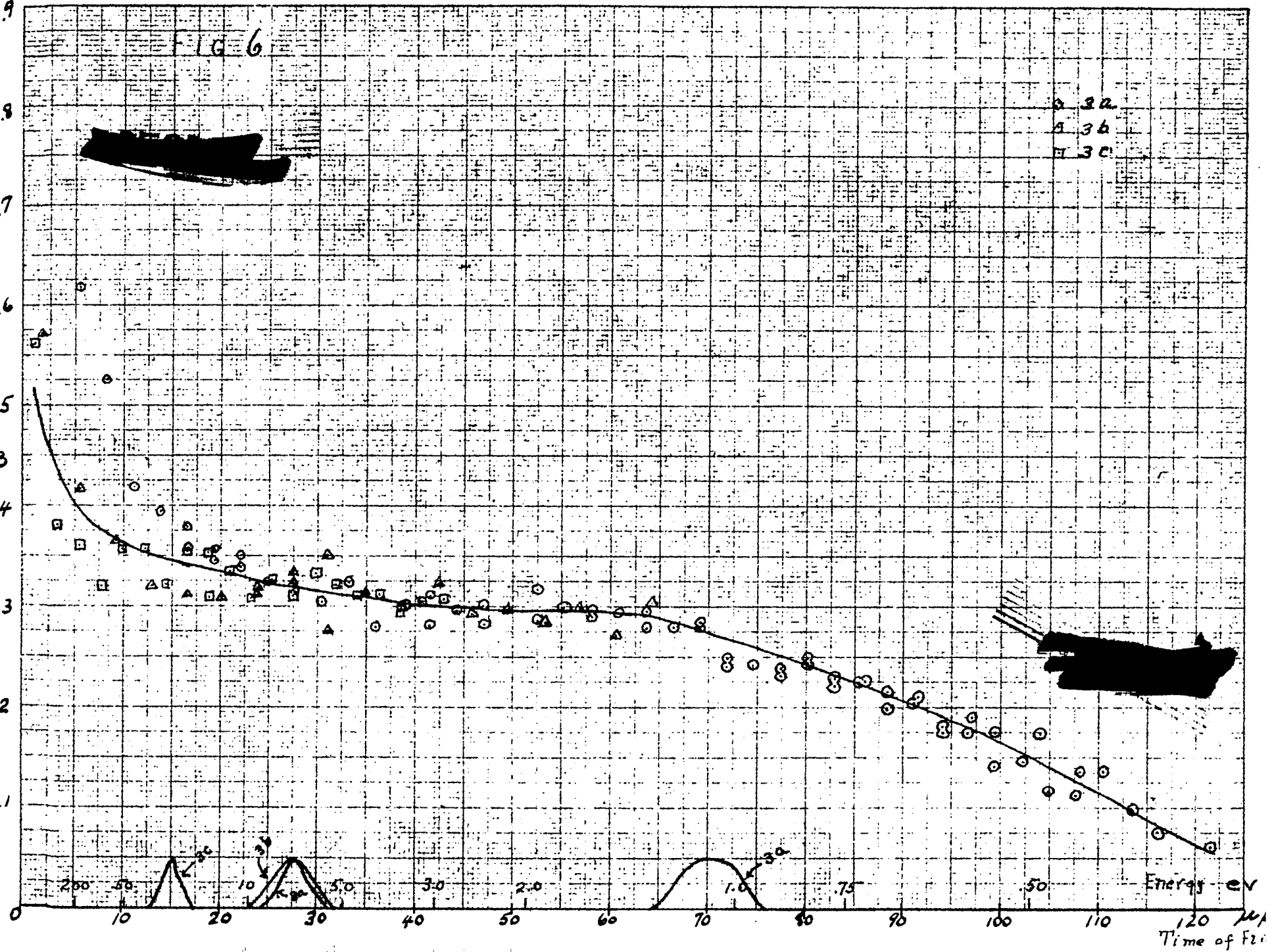
$\left(\frac{C}{T}\right)_B$

APPROVED FOR PUBLIC RELEASE

APPROVED FOR PUBLIC RELEASE

196

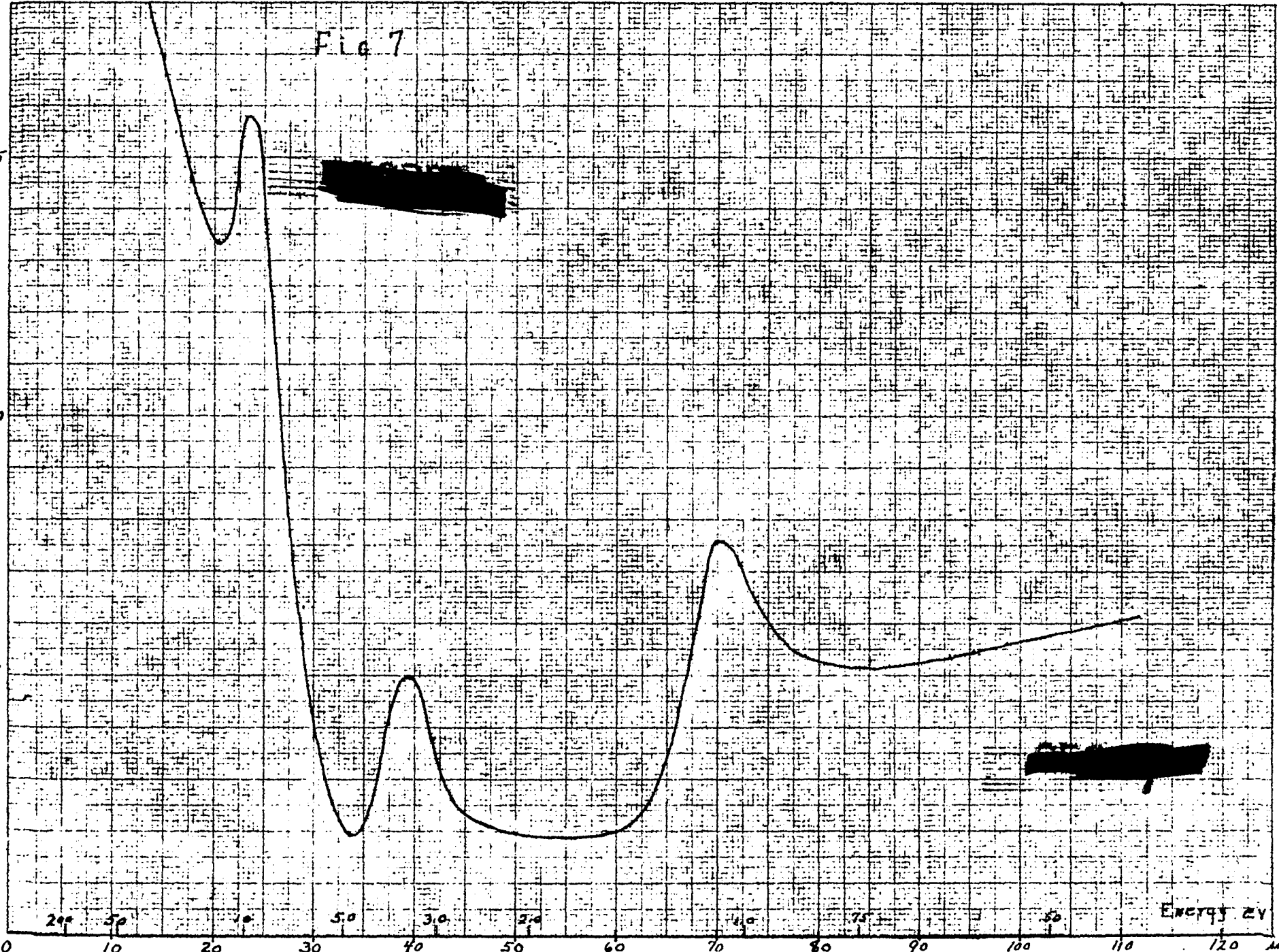
32
36
30



Energy - eV
Time of Exp. μs

$\frac{I_{25}}{I_0}$

Fig. 7



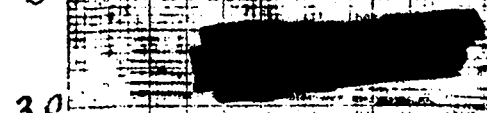
APPROVED FOR PUBLIC RELEASE

APPROVED FOR PUBLIC RELEASE

Energy eV

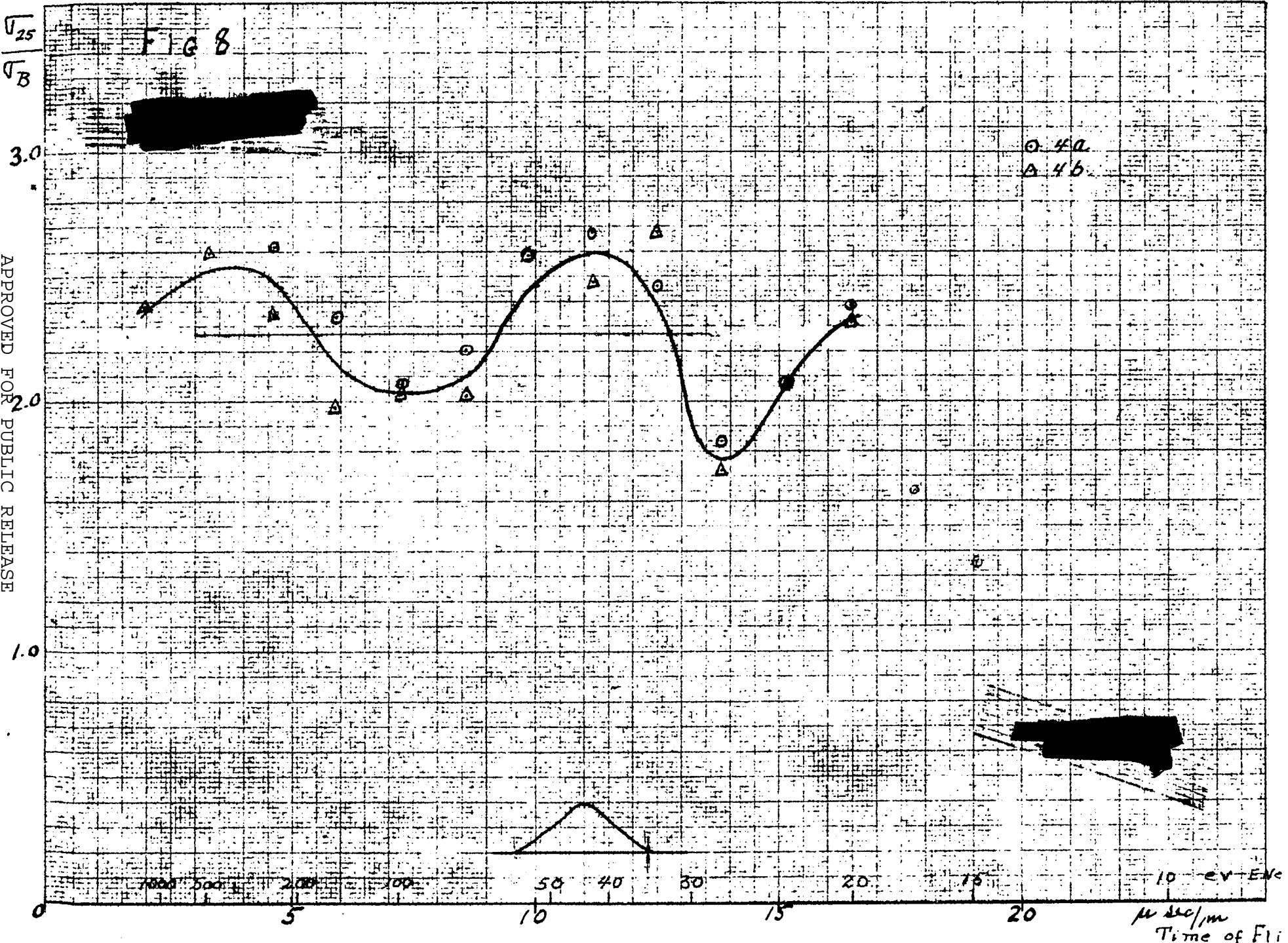
25
B

FIG 8

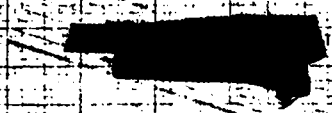


○ 4a.
△ 4b.

APPROVED FOR PUBLIC RELEASE



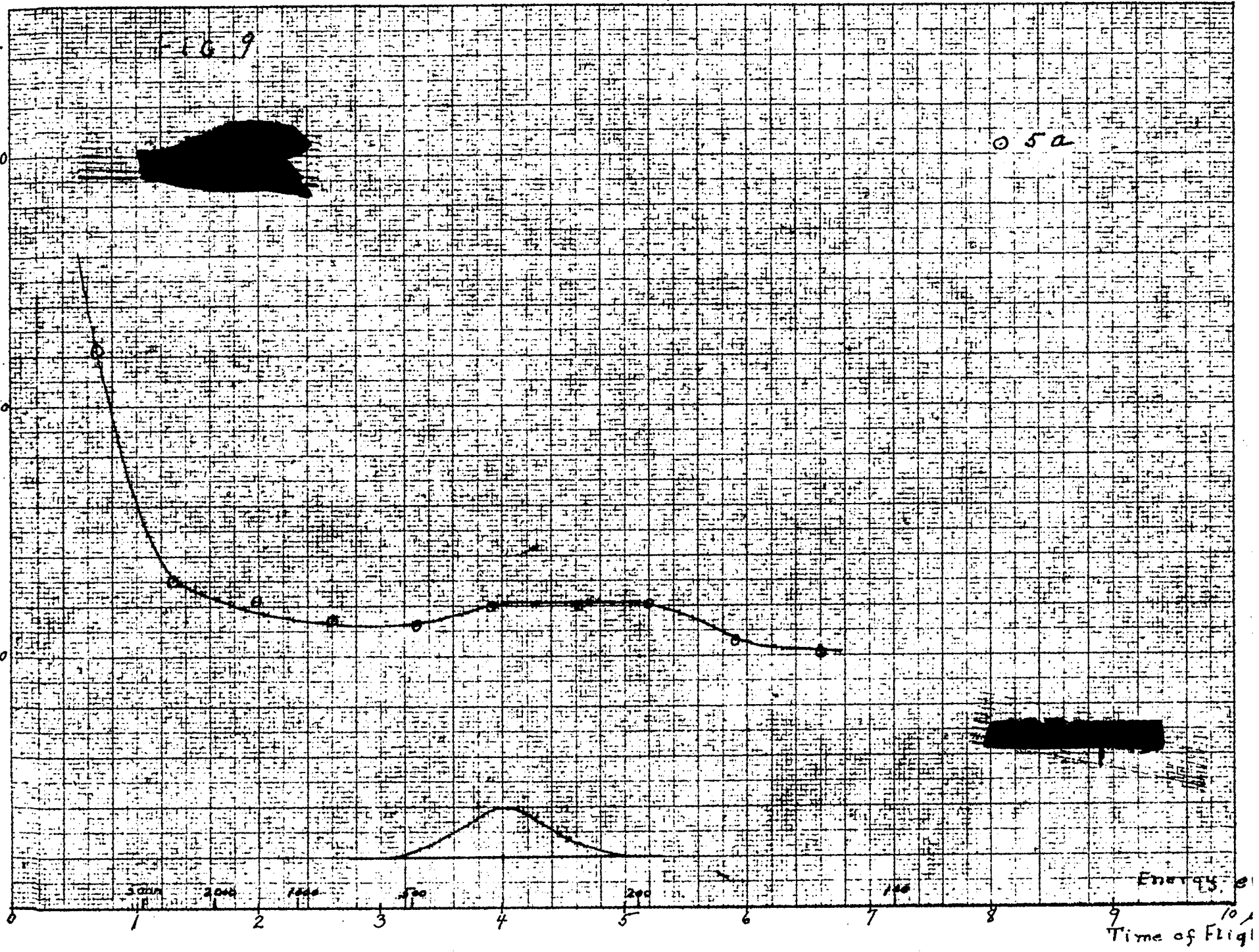
APPROVED FOR PUBLIC RELEASE



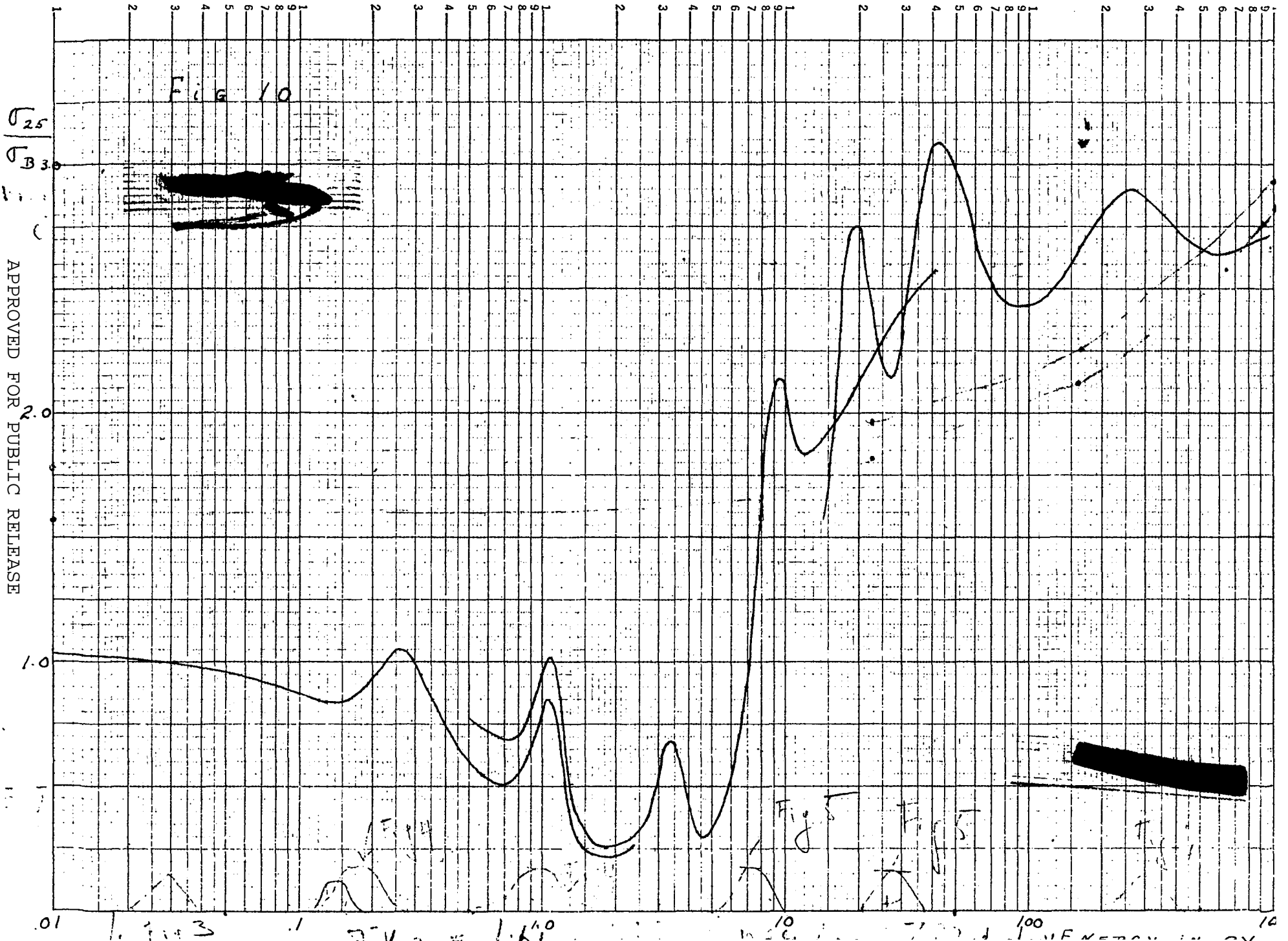
10 EV-ENC
μ sec/cm
Time of Flight

$\frac{L_{25}}{L_0}$

APPROVED FOR PUBLIC RELEASE



APPROVED FOR PUBLIC RELEASE



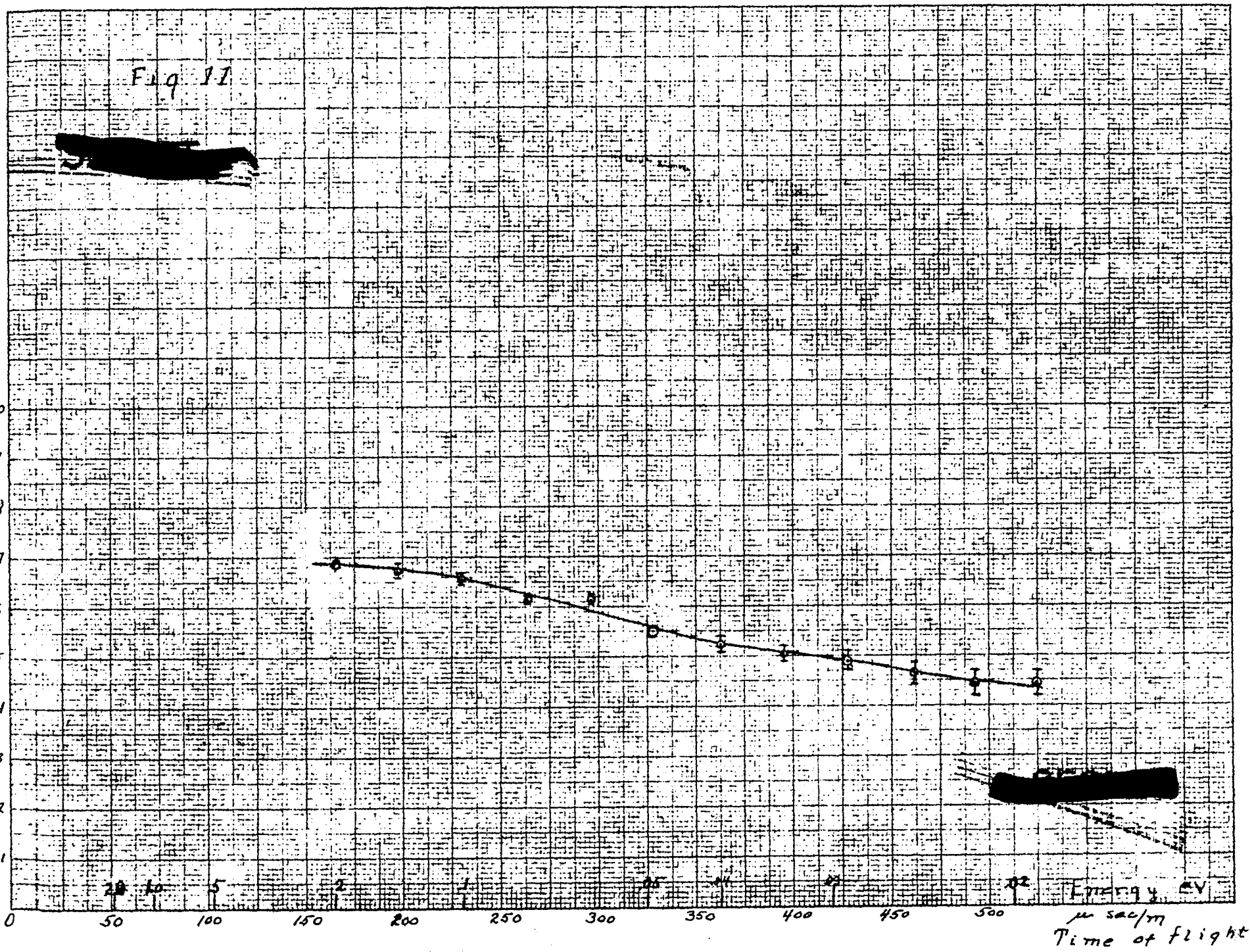
APPROVED FOR PUBLIC RELEASE

APPROVED FOR PUBLIC RELEASE

Fig 11

of counts

APPROVED FOR PUBLIC RELEASE



Energy, eV

Time of flight

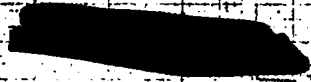
APPROVED FOR PUBLIC RELEASE

Fig 12

of coincidences

10
9
8
7
6
5
4
3
2
1

0 50 100 150 200 250 300 350 400 450 500 μ sec/m Energy ev
Time of flight

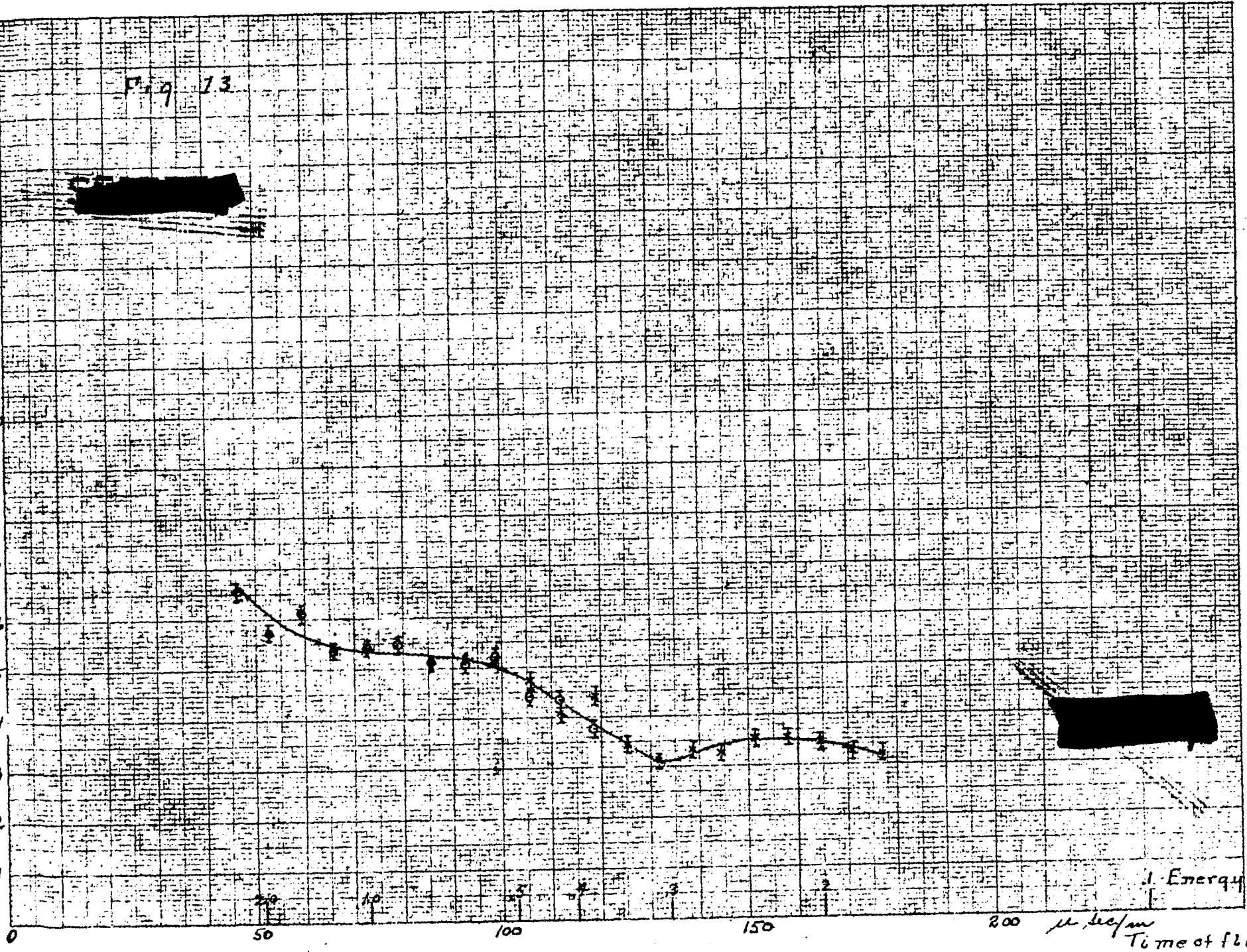


APPROVED FOR PUBLIC RELEASE

APPROVED FOR PUBLIC RELEASE

Fig. 13

Impedance to Coaxial Cable



APPROVED FOR PUBLIC RELEASE

APPROVED FOR PUBLIC RELEASE

Energie
Time of flight

APPROVED FOR PUBLIC RELEASE

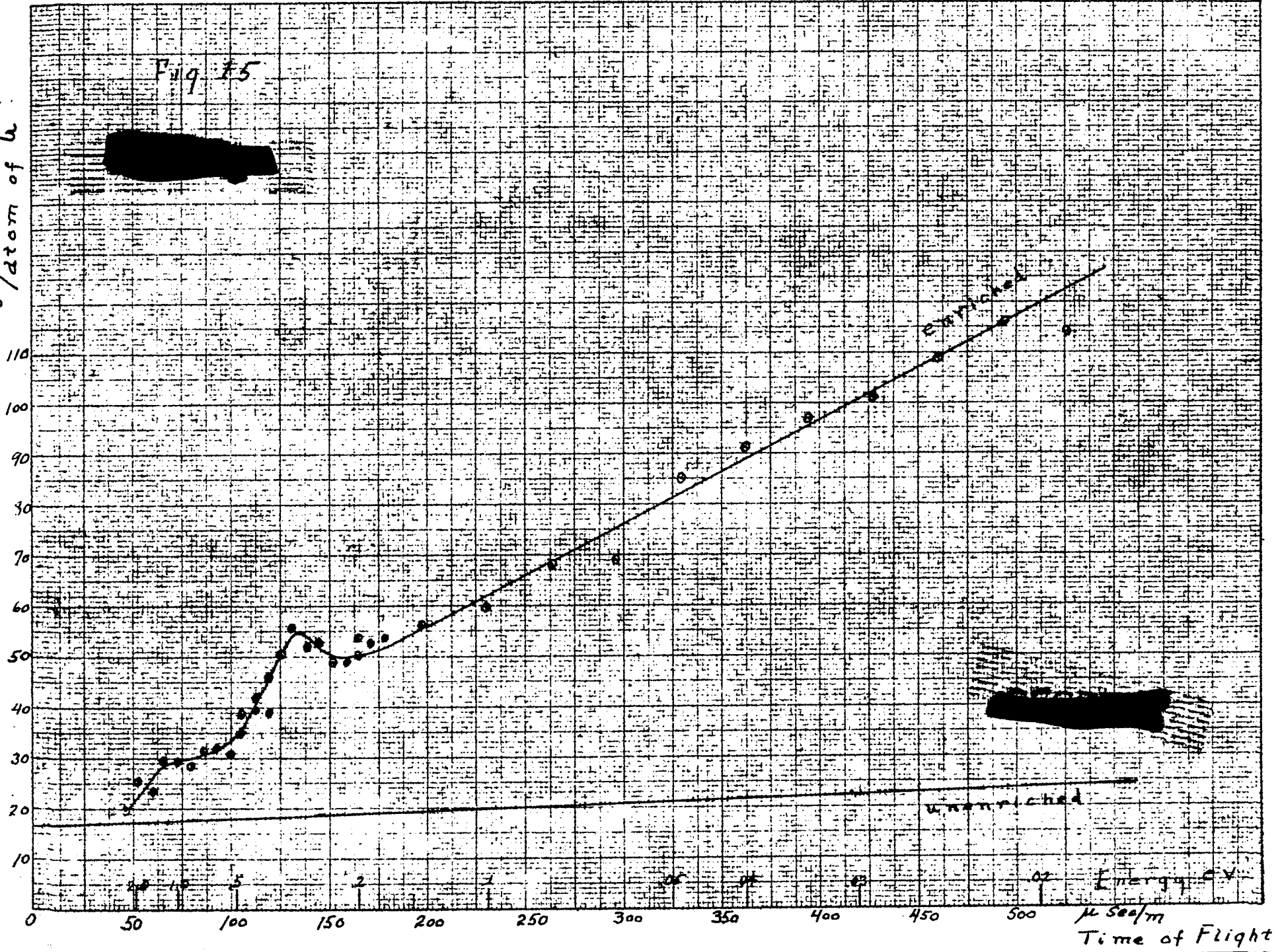
APPROVED FOR PUBLIC RELEASE



Fig. 15

η of $m\omega^2/d$

APPROVED FOR PUBLIC RELEASE

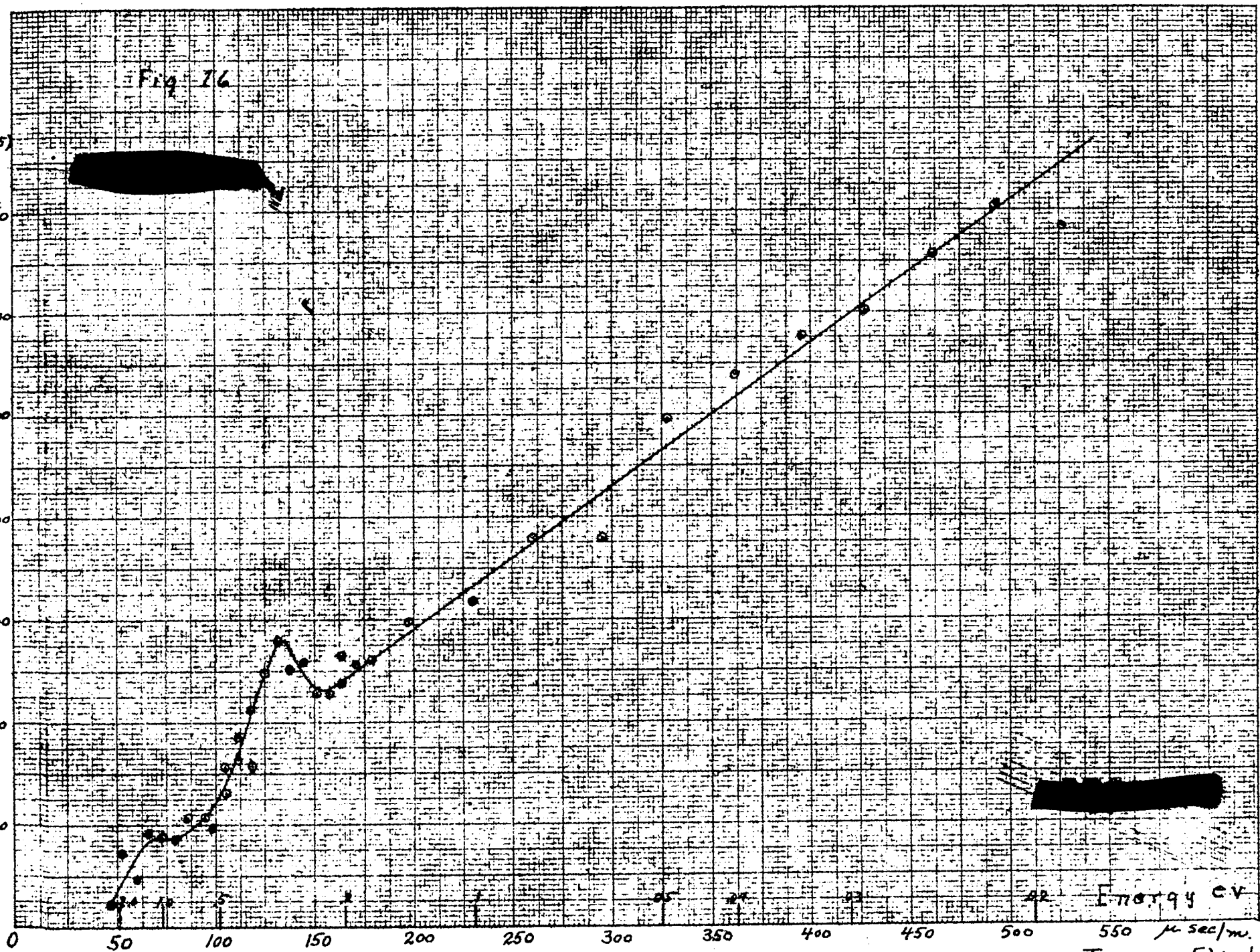


APPROVED FOR PUBLIC RELEASE

Fig. 76

$\sigma_c(25)$

APPROVED FOR PUBLIC RELEASE



Energy eV

Time of Flight

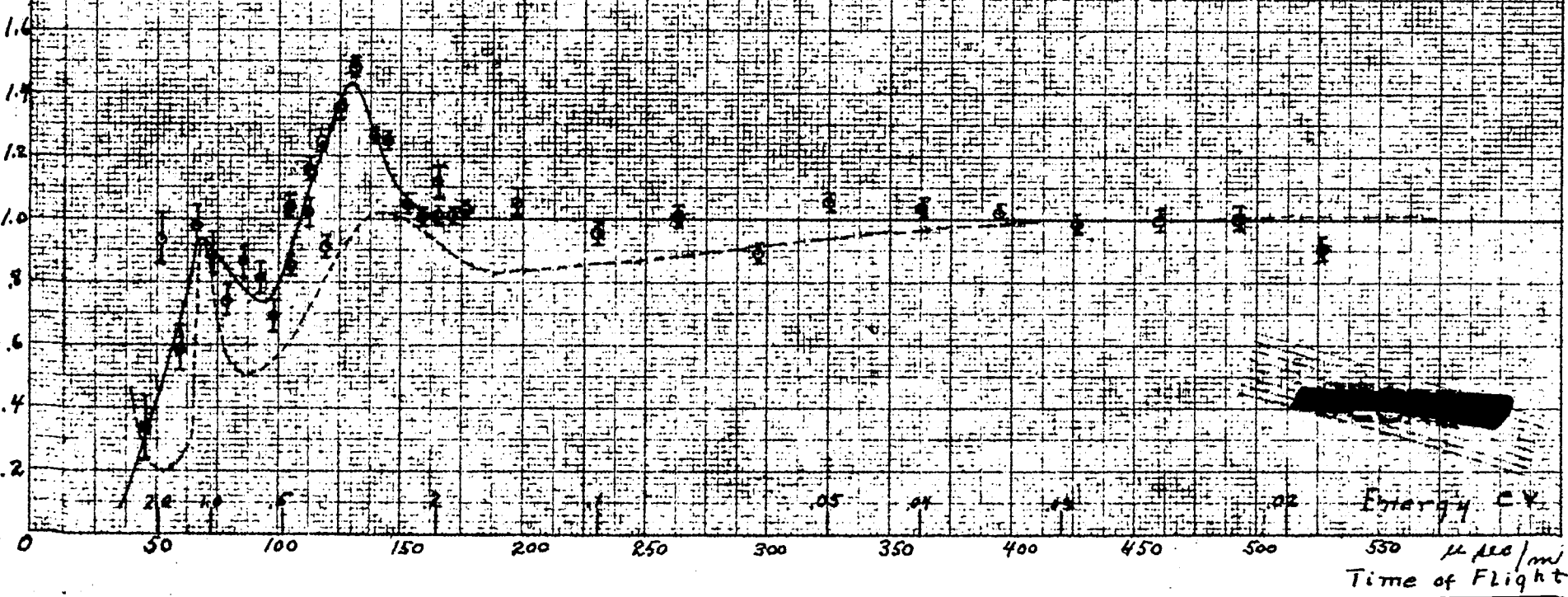
APPROVED FOR PUBLIC RELEASE

F-19-27



APPROVED FOR PUBLIC RELEASE

APPROVED FOR PUBLIC RELEASE



Energy CY
Time of Flight
 $\mu sec/mi$

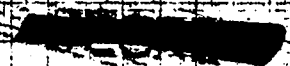
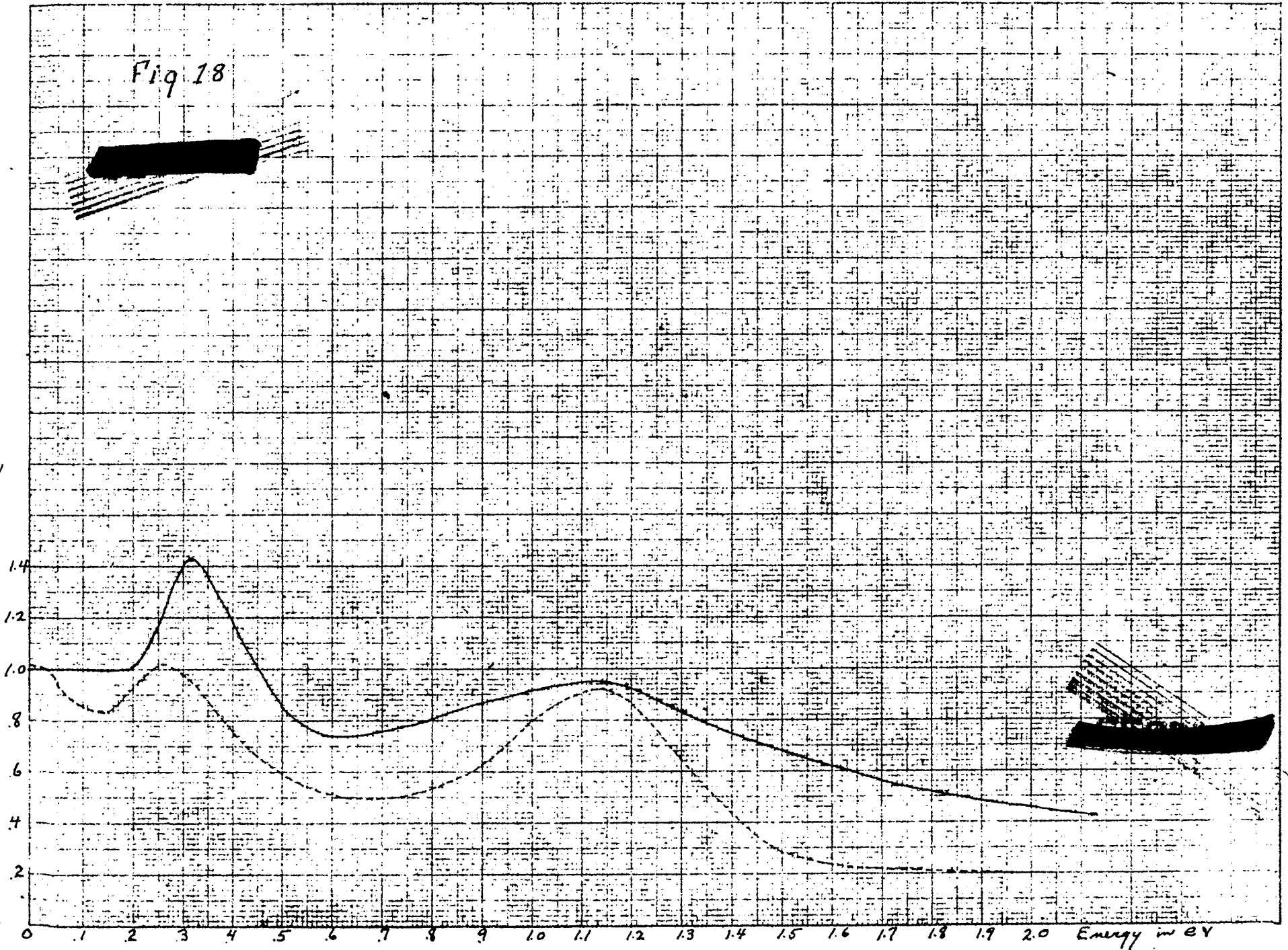


Fig 18



APPROVED FOR PUBLIC RELEASE

APPROVED FOR PUBLIC RELEASE

UNCLASSIFIED

REC. FROM C. J. BEE

DATE 10/11/57

REC. NO. REC.

UNCLASSIFIED